# Hydrodynamic model for sum and difference frequency generation at metal surfaces

Jesús A. Maytorena
*Facultad de Ciencias, Universidad Autónoma del Estado de Morelos, Avenida Universidad 1001, 62210 Cuernavaca, Morelos, Mexico*

W. Luis Mochán
*Instituto de Física, Universidad Nacional Autónoma de México, Apartado Postal 48-3, 62251 Cuernavaca, Morelos, Mexico*

Bernardo S. Mendoza
*Centro de Investigaciones en Optica. Apartado Postal 1-948, 37000 León, Guanajuato, Mexico*
(Received 9 April 1997; revised manuscript received 22 May 1997)

We develop a hydrodynamic model for the calculation of sum and difference frequency generation (SFG/DFG) at the surface of nonlocal conductors with arbitrary equilibrium electronic density profiles $n_0$. We apply our model to simple profiles and calculate the nonlinear surface susceptibility tensor $\chi^s_{zzz}(\omega_1,\omega_2)$ and the radiated efficiency $\mathcal{R}(\omega_3=\omega_1\pm\omega_2)$ as a function of the pump frequencies $\omega_1$ and $\omega_2$. $\mathcal{R}$ is strongly enhanced due to the excitation of the dipolar surface plasmon characterized by a resonant frequency $\omega_d$; it displays ridges whenever $\omega_1$, $\omega_2$, or $\omega_3\approx\omega_d$, an additional ridge at the bulk plasma frequency $\omega_3\approx\omega_b$, and very large double resonance peaks whenever two ridges cross each other. These results suggest that SFG/DFG spectroscopy might be a useful probe of surface collective modes. [S0163-1829(98)03403-1]

## I. INTRODUCTION

Optical second-order nonlinear spectroscopies such as second-harmonic generation (SHG) have been used widely to study surface and interface phenomena in centrosymmetric systems,[1–5] as the bulk contribution to the nonlinear signal is strongly suppressed. Very versatile surface probes have been based on sum and difference frequency generation (SFG/DFG), in which photons of frequencies $\omega_1$ and $\omega_2$ are mixed at an interface to yield photons of frequencies $\omega_3=\omega_1\pm\omega_2$, allowing the independent variation of the frequency and polarization of both incoming and/or the outgoing beams.[6–14] Although surface SFG has been employed for a decade,[15,16] its theoretical understanding is only now emerging.[17,18] In a previous paper[19] we have developed two simple models to calculate approximate SFG/DFG efficiency spectra for conductors and for dielectrics in terms of their linear dielectric response. The only relevant characteristic length scale in those models is the width of the selvedge, which, being much smaller than the wavelength of light, disappears from the final results. Therefore, those models predict a SFG/DFG signal that is independent of the molecular density profile at the surface of an insulator and of the electronic density profile at the surface of a conductor. The latter result cannot be generally correct, as it is known that the surface nonlinear susceptibility of a metal does depend quite strongly on the details of the electronic distribution[20,21] in the degenerate case of SHG. The origin of this failure lies in the spatial dispersion or nonlocality of the conductors response.[22] The electronic density and current induced at any position within a nonlocal conductor depend, even in the linear regime, on the exciting field at other neighboring positions. This yields additional length scales, such as the nonlocality range, the finite screening length, and the plasmon wavelength, which are typically of the order of the selvedge's width.

Most of the theoretical work on the SHG at metal surfaces has employed the jellium model, for which the surface is characterized by only two parameters $a(\omega)$ and $b(\omega)=-1$ and the bulk by a single parameter $d(\omega)=1$.[23–25] The former is related to the surface susceptibility $\chi^s_{zzz}$, where $z$ denotes the direction normal to the surface. This is the only component that is affected by the spatial dispersion of the metal[23,25] within the jellium model. As this model cannot explain the azimuthal anisotropy of the SHG signal,[26–30] several attempts have been made to incorporate crystallinity effects.[31–36] It has been shown that different components of the surface[33–36] response are characterized by different length scales whose relation to surface sensitivity is nontrivial, i.e., sensitivity not always decreases with increasing length scale. For example, while both the current $j_z(z)$ that contributes to $\chi^s_{zzz}$ and the current $j_x(z)$ that contributes to $\chi^s_{xzx}$ have a small decay length, of the order of the screening length, the former is very sensitive to the surface density profile while the latter is not. On the other hand, although the current $j_x(z)$ that contributes to $\chi^s_{xxx}$ in a crystalline metal surface such as Al(111) has a relatively large decay length, determined by that of the Friedel oscillations and by the nature of the electron states near the band gaps, it is very sensitive to the surface topography.[33–36] Similar effects are expected in the SFG and DFG surface response of nonlocal conductors.

As a first step to explore the effects of spatial dispersion on SFG/DFG, in the present paper we develop a hydrodynamic theory for the nonlinear response of a conductor with a conduction electron gas described by a continuous density profile. This constitutes a natural extension of a previous work[37] on SHG and it is the most simple model that incorporates nonlocal effects such as a finite screening length and the excitation of surface collective modes in the calculation of $\chi^s_{zzz}(\omega_1,\omega_2)$ for a centrosymmetric semi-infinite jellium.

 

Together with the other components of the surface susceptibility[17–19] we also calculate the SFG/DFG efficiency spectra.

The paper is organized as follows: In Sec. II we develop the hydrodynamic (HD) model to second order in a perturbing external field for an inhomogeneous electron gas. For this purpose we start from the equations of continuity and of momentum conservation. The boundary conditions obeyed by the induced first- and second-order polarization are obtained from the HD equations themselves. In Sec. III we present a calculation of the nonlinear surface parameter $a(\omega_1,\omega_2)$ which parametrizes $\chi^s_{zzz}$. We perform this calculation for a density profile that yields a multipolar surface plasmon at the expected energy.[38,39] We also calculate the SFG and DFG efficiency spectra and show that large structures are to be expected at resonance with the multipolar surface plasmon frequencies, suggesting an optical approach to the observation of these modes. Finally, Sec. IV is devoted to conclusions.

## II. THEORY

Our model system is a semi-infinite nonlocal jellium occupying the region $z>0$ with a nominal surface at the $xy$ plane. All the components of the bulk and surface quadratic susceptibility for this system are known,[17,19] as they may be obtained from a local theory, except for the normal component of the surface susceptibility $\chi^s_{zzz}$ on which we concentrate our attention. We assume that the selvedge's width is much less than an optical wavelength, so that we may perform our calculation in the nonretarded regime and ignore the fields variations along the surface.[40] For simplicity, we employ a hydrodynamic approach to calculate the linear and nonlinear surface response. We start the calculation from the continuity equation and from Euler's equation for momentum conservation in a semi-infinite electron fluid of density $n(z,t)$ and velocity field $u(z,t)\hat{z}$ in the presence of an electric field $E(z,t)\hat{z}$,

$$\partial_t n+\partial_z(nu)=0, \tag{1}$$

$$mn\partial_t u+mnu/\tau+mnu\partial_z u=-neE-\partial_z p(n). \tag{2}$$

The consecutive terms of Eq. (2) correspond to inertial forces, dissipation through friction with the positive background, convective momentum flow, electric force, and a pressure gradient. We took the charge of the electron as $-e$. We calculate the pressure $p$ starting from the density dependence of the average energy of a fermion within a noninteracting homogeneous gas $U/N=\frac{9}{10}\gamma n^{2/3}$, where $\gamma=(3\pi^2)^{2/3}\hbar^2/(3m)$. Then, assuming local equilibrium, the pressure is

$$p(n)=n^2\frac{\partial(U/N)}{\partial n}=\frac{3}{5}\gamma n^{5/3}(z,t), \tag{3}$$

as in the Thomas-Fermi theory. We account partially for the Coulomb interaction identifying $E$ as the self-consistent mean field and we neglect exchange and correlation.[41]

We perturb the system with a homogeneous external field $\vec{D}=(D_1e^{-i\omega_1 t}+D_2e^{-i\omega_2 t})\hat{z}+\text{c.c.}$ that oscillates at two frequencies $\omega_1$ and $\omega_2$, and we write all time-dependent quantities $f$ as a superposition of monochromatic waves with frequencies $n_1\omega_1+n_2\omega_2$ with integer $n_1$ and $n_2$,

$$\begin{aligned}f(z,t)=f_0(z)&+f(z,\omega_1)e^{-i\omega_1 t}+f(z,\omega_2)e^{-i\omega_2 t}\\&+f(z,2\omega_1)e^{-i2\omega_1 t}+f(z,2\omega_2)e^{-i2\omega_2 t}\\&+f(z,\omega_1+\omega_2)e^{-i(\omega_1+\omega_2)t}\\&+f(z,\omega_1-\omega_2)e^{-i(\omega_1-\omega_2)t}+\cdots+\text{c.c.},\end{aligned} \tag{4}$$

where $f(z,\omega_i)\equiv f_i(z)$ stands for either $n$, $u$, or $E$, and c.c. denotes the complex conjugate of the previous terms. Substituting in Eq. (2) and expanding the result in powers of the external field we generate a series of equations for the field variables. The zeroth- and first-order resulting equations are similar to those previously discussed in Ref. 37. The second-order equations include SHG at frequencies $2\omega_1$ and $2\omega_2$ which was also discussed in Ref. 37, and a new equation for SFG, namely,

$$\begin{aligned}\frac{\gamma}{m}n_0(z)\partial_z\{[n_0(z)]^{-1/3}\partial_z P_3(z)\}+[\Omega_3^2-\omega_p^2(z)]P_3(z)\\=S_3(z),\end{aligned} \tag{5}$$

where $P_3$ is the second-order contribution to the polarization oscillating at the sum frequency $\omega_3\equiv\omega_1+\omega_2$. The source of $P_3$,

$$\begin{aligned}S_3=&\frac{\gamma}{3me}n_0\partial_z[n_0^{-4/3}(\partial_z P_1)(\partial_z P_2)]+\frac{\omega_1\omega_2}{en_0}\partial_z(P_1P_2)\\&+\frac{\omega_1+\omega_2+i/\tau}{en_0}(\omega_2P_2\partial_z P_1+1\leftrightarrow 2)\\&-\frac{2\omega_1\omega_2}{en_0^2}P_1P_2\partial_z n_0,\end{aligned} \tag{6}$$

arises from the spatial derivatives of the equilibrium density $n_0$ and from the products $P_1P_2$ of the linear polarization at the fundamental frequencies. Here, we introduced the equilibrium density $n_0(z)$, the local plasma frequency $\omega_p(z)$, $\omega_p^2(z)=\omega_b^2n_0(z)/n_b$ where $\omega_b^2=4\pi n_b e^2/m$ and $n_b$ corresponds to the bulk plasmon frequency and density, respectively, and we abbreviated $\Omega_i^2\equiv\omega_i(\omega_i+i/\tau)$.

Using the analytical solution for the linear polarization $P_1$ and $P_2$ [Eq. (17) of Ref. 37],

$$P_i(z)=P_{ib}+A_ie^{iq_iz},\quad i=1,2 \tag{7}$$

in the bulk region where $n_0(z)=n_b$ is independent of $z$, the second-order differential equation (5) can be solved analytically,

$$\begin{aligned}P_3(z)=A_3e^{iq_3z}+\frac{i}{en_b\beta_b^2}\Bigg[&\frac{\mu_1q_1+\mu_2q_2}{q_3^2-(q_1+q_2)^2}A_1A_2e^{i(q_1+q_2)z}\\&-\left(\frac{\nu_1q_1P_{2b}}{q_3^2-q_1^2}A_1e^{iq_1z}+1\leftrightarrow 2\right)\Bigg],\end{aligned} \tag{8}$$

and it can be integrated numerically near the surface, where $n_0(z)$ varies from 0 in vacuum to its bulk value $n_b$. Here,

$\beta_b^2=(\gamma/m)n_b^{2/3}$, $\nu_i=-(\omega_3-\omega_i)(\omega_i+\omega_3+i/\tau)$, $\mu_i=\frac{1}{3}[2(\omega_3-\omega_i)(\omega_3-\omega_i+i/\tau)+6\omega_1\omega_2+\omega_b^2]$, $P_{ib}=(\epsilon_i-1)D_i/4\pi\epsilon_i$ is the bulk polarization linearly induced by $D_i$ in a local medium with a Drude dielectric response $\epsilon_i\equiv\epsilon(\omega_i)=1-\omega_b^2/\Omega_i^2$, and $q_i^2=(\Omega_i^2-\omega_b^2)/\beta_b^2$. The coefficients $A_1$, $A_2$, and $A_3$ are to be determined by sewing together the bulk and surface solutions using additional boundary conditions (ABC's). In the spirit of consistency within the HD model, as mentioned above, we derive the ABC's nonambiguously from the differential equations themselves. The linear boundary conditions[42,37] are the continuity of both $P_i$ and $n_0^{-1/3}\partial_z P_i$. These are equivalent to the ABC's first proposed by Forstmann and Stenschke[43] in order to satisfy energy and charge conservation at sharp boundaries between homogeneous layers. The second-order boundary conditions for the SH are given in Ref. 37 and were first obtained by Corvi and Schaich[44] from energy considerations. Demanding that the singularities that may be present on both sides of Eq. (5) should be of the same order leads immediately to the second-order ABC's for SF fields

$$P_3 \quad \text{continuous}, \tag{9}$$

$$(n_0^{-1/3}\partial_z P_3)-\frac{1}{3en_0^{2/3}}(n_0^{-1/3}\partial_z P_1)(n_0^{-1/3}\partial_z P_2)$$

$$-\frac{m\omega_1\omega_2}{e\gamma n_0^2}P_1P_2 \quad \text{continuous}. \tag{10}$$

After solving Eq. (5) to obtain $P_3(z)$ for a given profile $n_0(z)$ we calculate the surface nonlinear SF polarizations[45]

$$P_3^s\equiv\int dz P_3(z), \tag{11}$$

from which we identify the surface susceptibility

$$\chi_{zzz}^s(\omega_1,\omega_2)=P_3^s/(D_1D_2), \tag{12}$$

which is finally written in terms of a dimensionless parameter $a(\omega_1,\omega_2)$, defined by[17,19]

$$\chi_{zzz}^s(\omega_1,\omega_2)=-\frac{a(\omega_1,\omega_2)}{2n_be}\frac{\epsilon_1-1}{4\pi\epsilon_1}\frac{\epsilon_2-1}{4\pi\epsilon_2}. \tag{13}$$

With $a(\omega_1,\omega_2)$ it is a simple matter to calculate the SFG efficiency $\mathcal{R}$.[17,19] For this we also need the other non-null components of the nonlinear surface susceptibilities $\chi_{\|z\|}^s$ and $\chi_{\|\|z}^s$, and the nonlinear response of the bulk. We parametrize these through the dimensionless functions introduced in Refs. 17 and 19: $b(\omega_1,\omega_2)=\underline{b}(\omega_2,\omega_1)=-1$ for the surface response, and $d_1=d_2=\underline{d}_1=\underline{d}_2=1$ for the bulk response.

Finally, we remark that DFG, i.e., $\omega_3=\omega_1-\omega_2$, may be calculated from the results of the present section for SFG, i.e., $\omega_3=\omega_1+\omega_2$ by the simple replacement $\omega_2\leftarrow-\omega_2$.

## III. RESULTS

Previous works[46] on the applicability of the HD model to the calculation of the linear optical response of the inhomogeneous electron gas warned against its use since it yields spurious collective modes originated in the exponentially decaying tail of the electron gas density profile;[47] they recommended the use of less realistic profiles which go to zero at some well-defined point. Then, to illustrate our model we consider a simple linear shape for the equilibrium density profile $n_0(z)$ that interpolates between its vacuum and bulk values,

$$n_0(z)=\begin{cases} n_b, & z>z_s \\ \dfrac{n_b}{2}(1+z/z_s), & -z_s<z<z_s \\ 0, & z<-z_s, \end{cases} \tag{14}$$

where $z_s$ is the width of the selvedge region. We will consider parameters that correspond roughly to potassium: we chose the bulk density parameter $r_s=4.86a_0$ ($n_b^{-1}\equiv 4\pi r_s^3/3$, $a_0$ is Bohr's radius), and we took $\omega_b\tau=10$.[48] We took a larger dissipation than that expected within the bulk in order to account approximately for surface damping mechanisms which are not present explicitely in our model. As shown in Ref. 37, the linear response shows a resonance corresponding to the usual bulk plasmon at $\omega_i=\omega_b$, and a number of resonances whose induced densities have a multipolar character. Their number, position, and strength depend on the width of the selvedge. Therefore, we have adjusted the width parameter $z_s=3.5a_0$ to yield a single peak of dipolar character close to the experimentally measured frequency $\omega_d=0.8\omega_b$.[38,39] Having adjusted our model to reproduce qualitatively the main features of the surface linear response,[49,48,50] we have exhausted the single free parameter of our model. We remark that, as in Ref. 37, the parameter $a$ is independent and the efficiency $\mathcal{R}$ is inversely proportional to the bulk density for a given dimensionless width $\zeta_s=z_s/\lambda_{\mathrm{TF}}$, with $\lambda_{\mathrm{TF}}=\beta_b/\omega_b$ the Thomas-Fermi screening length, if the frequencies and lifetimes are scaled with $\omega_b$. Now, we proceed to perform the nonlinear part of our calculation.

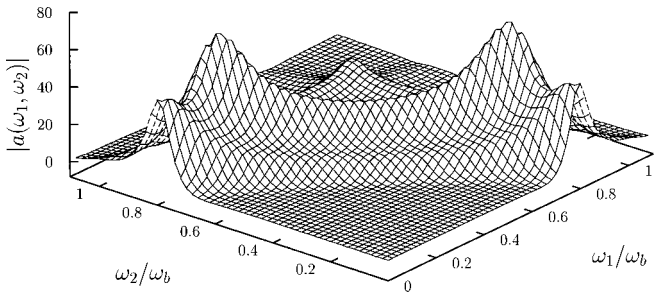


FIG. 1. Absolute value of $a(\omega_1,\omega_2)$ for SFG vs $\omega_1/\omega_b$ and $\omega_2/\omega_b$, for K ($r_s=4.86a_0$) with a linear surface density profile. The parameters are: $\omega_b\tau=10$ and selvedge width $z_s=3.5a_0$. Notice that $a$ is independent of $r_s$.

Figure 1 shows our numerical results for the surface parameter $|a(\omega_1,\omega_2)|$ as a function of the fundamental frequencies $\omega_1$ and $\omega_2$. There are ridges corresponding to constant values of $\omega_1=\omega_d$, $\omega_2=\omega_d$, $\omega_3=\omega_d$, and $\omega_3=\omega_b$. Since our model doesn't incorporate single particle excitations, our results do not display any structure related to the photoionization threshold.[21] Curiously, there is no peak corresponding to $\omega_1$ or $\omega_2=\omega_b$ due to the factors $\epsilon_1$ and $\epsilon_2$ in

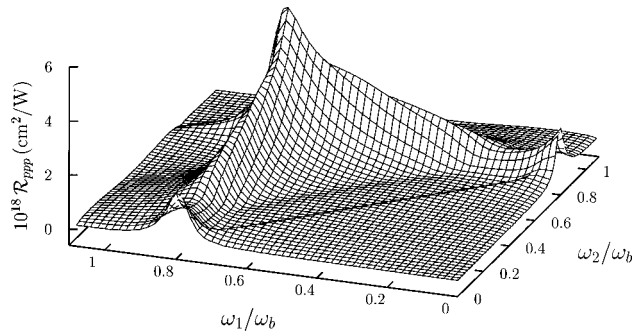


FIG. 2. $p$-polarized SFG efficiency $\mathcal{R}_{ppp}(\omega_1,\omega_2)$ for two $p$-incoming fundamental beams at equal angles of incidence $\theta_1=\theta_2=60°$, for the same system as in Fig. 1. The results for other metals can be obtained by multiplying $\mathcal{R}_{ppp}$ by $[r_s/r_s(\mathrm{K})]^3$.

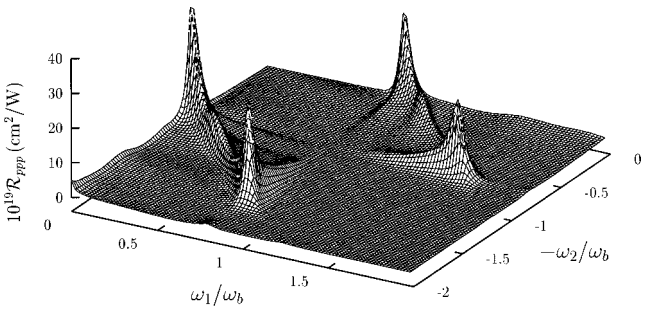


FIG. 4. $p$-polarized DFG efficiency $\mathcal{R}_{ppp}(\omega_1,-\omega_2)$ for two $p$-incoming fundamental beams at equal angles of incidence $\theta_1=\theta_2=60°$, for the same system as in Fig. 1. The results for other metals can be obtained by multiplying $\mathcal{R}_{ppp}$ by $[r_s/r_s(\mathrm{K})]^3$.

its definition [Eq. (13)]. When the ridges cross, the resulting double resonance yields strong enhancements. In particular, the peak at $\omega_1=\omega_2=\omega_d$ corresponds to SHG at the dipolar surface plasmon resonance $\omega_3=2\omega_d$. The peak previously obtained for SHG at the subharmonic of the dipolar surface plasmon[21,37] $\omega_1=\omega_2=\omega_d/2$ is seen in Fig. 1 to correspond only to a ridge crossing along the SHG line $\omega_1=\omega_2$, but is not actually a peak in the SFG landscape. In Fig. 2 we show the $p$-polarized SFG efficiency $\mathcal{R}_{ppp}$ for two incoming $p$-polarized fundamental beams at equal angles of incidence $\theta_1=\theta_2=60°$. We notice that the peaks and ridge visible in Fig. 1 at $\omega_3=\omega_b$ are suppressed due to the Fresnel factor involved in $\mathcal{R}_{ppp}$.[17,19] Now, we only have ridges at $\omega_1$ or $\omega_2=\omega_d$, and a much smaller ridge at $\omega_3=\omega_d$. However, the peaks at the dipolar-plasmon frequency are still very strong. If we traverse Fig. 2 along the degenerate $\omega_1=\omega_2$ line, we obtain the same SHG spectra reported in Ref. 37 but scaled by a factor of four.[18,19] Notice that Fig. 1 has the symmetry $\omega_1\leftrightarrow\omega_2$ which leaves $\omega_3$ invariant. Since we took $\theta_1=\theta_2$, Fig. 2 has the same symmetry; obviously the efficiency is symmetric under simultaneous permutation of the incoming frequencies, incidence angles, and polarizations.

Similarly we can obtain $a(\omega_1,\omega_2)$ for the case of difference frequency generation (DFG), for which $\omega_3=\omega_1-\omega_2$, since this case could be obtained from SFG by substituting $\omega_2\leftarrow-\omega_2$. For instance, we could define $a_{\mathrm{DFG}}(\omega_1,\omega_2)=a(\omega_1,-\omega_2)$ and employ similar definitions for the other DFG response functions. In Fig. 3, we show $|a(\omega_1,-\omega_2)|$ as a function of $\omega_1$ and $-\omega_2$. Again, we notice a series of ridges and large enhancements where the ridges cross each other. The ridges occur for constant values $\omega_1$ or $\omega_2=\omega_d$, and $\omega_3=\pm\omega_d$ or $\pm\omega_b$. The plot is symmetric with respect to the optical rectification line $\omega_3=0$, and actually, the region where $\omega_3$ is negative should be interpreted as the other DFG process $\omega_3'=\omega_2-\omega_1$, for which $a_{\mathrm{DFG}}(\omega_2,\omega_1)=a^*_{\mathrm{DFG}}(\omega_1,\omega_2)$. We obtain an optical rectification peak when both $\omega_1$ and $\omega_2=\omega_d$. In Fig. 4 we show the $p$-polarized DFG efficiency $\mathcal{R}_{ppp}$ for the same incoming beams as in Fig. 2. As before, we notice that the peaks and ridge visible in Fig. 3 at $\omega_3=\pm\omega_b$ are suppressed due to the Fresnel factor. The optical rectification peak vanishes identically since $\mathcal{R}_{ppp}$ is proportional to $\omega_3^2$. We only have ridges at $\omega_1$, $\omega_2=\omega_d$, or $\pm\omega_3=\omega_d$. In contrast to SFG, when computing the DFG efficiency, extreme care should be taken as it may happen that there is no real solution for the outgoing angle $\theta_3$ of the reflected beam for some combinations of angles of incidence and fundamental frequencies.[51] Whenever this is the case, no energy flows at $\omega_3$ from the surface towards vacuum and the expressions we employed for $\mathcal{R}_{ppp}$ are no longer valid. By taking $\theta_1=\theta_2$ in Fig. 4 we circumvent this problem. Also, concomitant with this choice, the results shown in Fig. 4 have the same symmetry as those shown in Fig. 3.

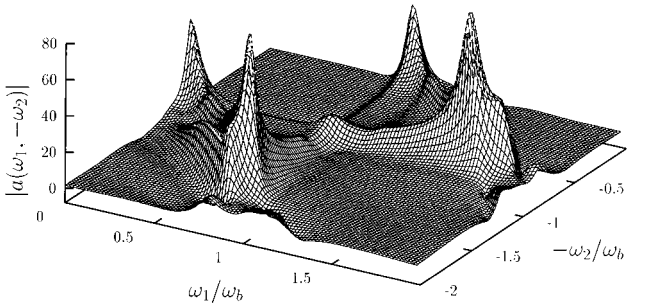


FIG. 3. Absolute value of $a(\omega_1,-\omega_2)$ for DFG vs $\omega_1/\omega_b$ and $-\omega_2/\omega_b$. The system is the same as in Fig. 1. Notice that $a$ is independent of $r_s$.

The resonant structure in SHG due to the excitation of multipolar surface plasmons has been predicted previously in Refs. 21 and 37, and the use of SHG spectroscopy to observe this elusive surface mode has been suggested. Our present results shows that SFG/DFG spectroscopy is also a feasible way to observe this mode.

The important spectral features presented above are consequence of the finite thickness of the selvedge region. On the other hand, for a single step density profile $[n_0(z)=n_b\Theta(z)]$, there is only one feature at $\omega_b$ and the spectra is otherwise featureless. This is easily seen from Eq. (5) and Eq. (11), which can be solved analytically to yield

$$a(\omega_1,\omega_2)=\frac{1}{q_3}\frac{2}{\beta_b^2}\left[\frac{\nu_1}{q_1+q_3}+\frac{\nu_2}{q_2+q_3}+\frac{\mu_1 q_1+\mu_2 q_2}{(q_1+q_2)(q_1+q_2+q_3)}\right]. \quad (15)$$

The only resonant structure is at $\omega_3=\omega_b$ and comes from the $1/q_3$ prefactor in Eq. (15).

## IV. CONCLUSIONS

In this paper we have developed a hydrodynamic model to calculate the linear and second-order surface response and the SFG/DFG efficiency of semiinfinite simple metals taking account of spatial dispersion and the presence of a continuous electronic density profile at their surface. Starting from the continuity and Euler's equation we obtained the first- and second-order equations for the induced polarization. From these equations we also obtained the boundary conditions to be imposed on the sum and difference frequency polarization. The hydrodynamic model overemphasizes the contributions to the response from the exponentially decaying tail, and is therefore unable to deal with realistic density profiles.[46] In this paper we employed a simple model profile that interpolates between the bulk density and vacuum. We chose the profile parameters so that the frequency of the linear surface response fitted the position of the dipolar surface collective mode, as obtained from self-consistent jellium calculations[48,50] and from experiment.[38,39]

By choosing the appropriate density, we calculated numerically the nonlinear susceptibility of potassium and discussed its normal-to-the-surface component, characterized by the $a(\omega_1,\omega_2)$ parameter. We also calculated its nonlinear reflectance $\mathcal{R}$. However, we remark that there are simple scaling laws that permit the immediate extrapolation of our numerical results to simple metals with a different bulk density. As in the case of SHG,[37] given a density profile shape, the surface is entirely characterized by the dimensionless parameter $\zeta_s = z_s/\lambda_{\mathrm{TF}} = 2.48$. Then the susceptibility parameter $a$ scales as $a(\omega_1,\omega_2) = \tilde{a}(\omega_1/\omega_b, \omega_2/\omega_b; \omega_b\tau, \zeta_s)$ and the efficiency scales as $\mathcal{R}(\omega_1,\omega_2) = [2/(n_b m c^3)]\tilde{\mathcal{R}}(\omega_1/\omega_b, \omega_2/\omega_b; \omega_b\tau, \zeta_s)$, where $\tilde{a}$ and $\tilde{\mathcal{R}}$ are dimensionless functions independent of the bulk density. In summary, $a$ is independent of the bulk density if the frequencies are scaled by the plasma frequency, and $\mathcal{R}$ scales with the inverse of the density.

The SFG efficiency $\mathcal{R}_{ppp}$ displays sharp peaks at resonance with the dipolar surface plasmon when $(\omega_1,\omega_2) = (\omega_d,0)$, $(0,\omega_d)$, and $(\omega_d,\omega_d)$. Similarly, the DFG efficiency shows peaks at $(\omega_1,-\omega_2) = (2\omega_d,-\omega_d)$, $(\omega_d,0)$ and similar peaks obtained by interchanging $\omega_1$ with $\omega_2$. The surface response $a(\omega_1,\omega_2)$ has the structure above, and extra structures due to resonances with the bulk plasma frequency. However, this extra structure disappears when calculating $\mathcal{R}_{ppp}$ due to the presence of the Fresnel factors. We stress that the directly observable quantity is $\mathcal{R}$ and not the surface response.

The ground-state density profile chosen for the calculations shown in the present paper was a simple linear interpolation between the bulk density and vacuum. Slightly more realistic profiles, such as a quadratic interpolation with a continuous derivative yield even larger peaks. Similar results for SHG were discussed in detail in Ref. 37. For our calculations we took a very large dissipation in order to account for possible surface damping effects that are not explicitly accounted for within our model. Had we taken a smaller dissipation $\omega_b\tau = 30$ (Ref. 48) the peak heights would have increased by two orders of magnitude, concealing the ridge structure.

The results obtained in the paper strongly suggest that the multipolar modes, which are difficult to observe in electron scattering experiments, might be observed through SFG/DFG spectroscopy. Since there is more freedom in the choice of input parameters, their observation using SFG/DFG may be more feasible than with SHG. For instance, the peaks at $\omega_1 = \omega_d$ and $\omega_2 = 0$ in Figs. 2 and 4 may be explored with ultraviolet-infrared SFG/DFG, while SHG displays a large peak at $\omega_1 = \omega_2 = \omega_d$ which would require detection optics far within the ultraviolet region. The SHG peak at $\omega_1 = \omega_2 = \omega_d/2$ is much smaller and actually corresponds only to a pass in the $\omega_3 = \omega_d$ SFG ridge.

In summary, we have presented a calculation of the surface SFG and DFG spectra of simple metals taking into account the spatial dispersion of their optical response and the presence of a continuous ground-state density profile at their surface. We employed a simple hydrodynamic model for the inhomogeneous electron gas and fitted its free parameters to the position of the dipolar surface plasmon. The surface nonlinear susceptibility and its efficiency display a series of very large peaks corresponding to the excitation of multipolar surface plasmons, indicating that the observation of these elusive modes might be performed with SFG/DFG spectroscopy. Although the shortcomings of hydrodynamic models for the realistic description of metal surfaces are well known,[48] our parametrized model captures qualitatively some of the features of more elaborate models, such as a negative dispersion for the ordinary surface plasmon and the existence of a multipolar resonance. Others, such as those due to the photoemission threshold, are necessarily missing from our calculation, although they have appeared in more sophisticated calculations of SHG.[21] To our knowledge, ours are the first calculations of surface SFG and DFG spectra over a large frequency range for nonlocal metals, and we believe that the large predicted resonances will also be present in more elaborate calculations. We hope our calculation encourages more experiments to measure the SFG spectra, and more theoretical calculations close to the surface resonances.

## ACKNOWLEDGMENTS

We acknowledge the partial support of CONACyT-México 3246-E9308 (B.S.M.) and of DGAPA-UNAM (Grants Nos. IN107796 and IN104594) (W.L.M.).

[1] Y. R. Shen, Nature (London) **337**, 519 (1989).

[2] T. F. Heinz, in *Nonlinear Surface Electromagnetic Phenomena*, edited by H.-E. Ponath and G. I. Stegeman (North-Holland, Amsterdam, 1991), Chap. 5, p. 253.

[3] S. Janz and H. M. van Driel, Int. J. Nonlinear Opt. Phys. **2**, 1 (1993).

[4] Y. R. Shen, Surf. Sci. **299/300**, 551 (1994).

[5] G. A. Reider and T. F. Heinz, in *Photonic Probes of Surfaces*, edited by P. Halevi (North Holland, Amsterdam, 1995), Chap. 9, p. 413.

[6] A. L. Harris, C. E. D. Chidsey, N. Y. Levinos, and D. N. Loiacono, Chem. Phys. Lett. **141**, 350 (1987).

[7] A. L. Harris, L. Rothberg, L. H. Dubois, N. J. Levinos, and L. Dhar, Phys. Rev. Lett. **64**, 2086 (1990).
[8] P. Guyot-Sionnest, P. Dumas, Y. J. Chabal, and G. S. Higashi, Phys. Rev. Lett. **64**, 2156 (1990).
[9] Q. Du, R. Superfine, E. Freysz, and Y. R. Shen, Phys. Rev. Lett. **70**, 2313 (1993).
[10] A. Peremans and A. Tadjedine, Chem. Phys. Lett. **220**, 481 (1994).
[11] A. Peremans and A. Tadjedine, Phys. Rev. Lett. **73**, 3010 (1994).
[12] M. S. Yeganeh, S. M. Dougal, R. S. Polizzotti, and P. Rabinowitz, Phys. Rev. Lett. **74**, 1811 (1995).
[13] P. Cremer, C. Stanner, J. W. Niemantsverdriet, Y. R. Shen, and G. Somorjai, Surf. Sci. **328**, 111 (1995).
[14] K. A. Friedrich, W. Daum, C. Klunker, D. Knabben, U. Stimming, and H. Ibach, Surf. Sci. **335**, 315 (1995).
[15] X. D. Zhu, H. Suhr, and Y. R. Shen, Phys. Rev. B **35**, 3047 (1987).
[16] P. Guyot-Sionnest, J. H. Hunt, and Y. R. Shen, Phys. Rev. Lett. **59**, 1597 (1987).
[17] A. V. Petukhov, Phys. Rev. B **52**, 16901 (1995).
[18] A. V. Petukhov and T. Rasing, Surf. Sci. **377-379**, 414 (1997).
[19] Jesús A. Maytorena, Bernardo S. Mendoza, and W. Luis Mochán, preceding paper, Phys. Rev. B **57**, 2569 (1998).
[20] P. Guyot-Sionnest, A. Tadjeddine, and A. Liebsch, Phys. Rev. Lett. **64**, 1678 (1990).
[21] A. Liebsch and W. L. Schaich, Phys. Rev. B **40**, 5401 (1989).
[22] R. Fuchs and P. Halevi, in *Spatial Dispersion in Solids and Plasmas*, Electromagnetic Waves Vol. 1, edited by P. Halevi (North-Holland, Amsterdam, 1992), p. 1.
[23] J. Rudnick and E. A. Stern, Phys. Rev. B **4**, 4274 (1971).
[24] J. E Sipe, V. C. Y. So, M. Fukui, and G. I. Stegeman, Phys. Rev. B **21**, 4389 (1980).
[25] J. E. Sipe and G. I. Stegeman, in *Surface Polaritons*, edited by V. M. Agranovich and D. L. Mills (North-Holland, New York, 1982).
[26] H. W. K. Tom and G. D. Aumiller, Phys. Rev. B **33**, 8818 (1986).
[27] J. E. Sipe, D. J. Moss, and H. M. van Driel, Phys. Rev. B **35**, 1129 (1987).
[28] R. A. Bradley, S. Arekat, R. Georgiadis, J. M. Robinson, S. D. Levan, and G. L. Richmond, Chem. Phys. Lett. **168**, 468 (1990).
[29] S. Janz, K. Pedersen, and H. M. van Driel, Phys. Rev. B **44**, 3943 (1991).
[30] G. Lüpke, D. J. Bottomley, and H. M. van Driel, J. Opt. Soc. Am. B **11**, 33 (1994).
[31] A. V. Petukhov, Phys. Rev. B **42**, 9387 (1990).
[32] A. V. Petukhov and A. Liebsch, Surf. Sci. **294**, 381 (1993).
[33] A. V. Petukhov and A. Liebsch, Surf. Sci. **320**, L51 (1994).
[34] A. V. Petukhov and A. Liebsch, Surf. Sci. **334**, 195 (1995).
[35] A. V. Petukhov, Ch. Jakobsen, and K. Pedersen, Surf. Sci. **369**, 265 (1996).
[36] A. V. Petukhov, Surf. Sci. **347**, 143 (1996).
[37] J. A. Maytorena, W. Luis Mochán, and Bernardo S. Mendoza, Phys. Rev. B **51**, 2556 (1995).
[38] H. Levinson, E. W. Plummer, and P. J. Feibelman, Phys. Rev. Lett. **43**, 952 (1979).
[39] K.-D. Tsuei, E. W. Plummer, A. Liebsch, K. Kempa, and P. Bakshi, Phys. Rev. Lett. **64**, 44 (1990); K.-D. Tsuei, E. W. Plummer, A. Liebsch, E. Pehlke, K. Kempa, and P. Bakshi, Surf. Sci. **247**, 302 (1991).
[40] W. L. Schaich and A. Liebsch, Phys. Rev. B **37**, 6187 (1988).
[41] A. Chizmeshya and E. Zaremba, Phys. Rev. B **37**, 2805 (1988).
[42] M. del Castillo-Mussot, W. L. Mochán, and Bernardo S. Mendoza, J. Phys.: Condens. Matter **5**, A393 (1993).
[43] F. Forstmann and H. Stenschke, Phys. Rev. Lett. **38**, 1365 (1977); Phys. Rev. B **17**, 1489 (1978).
[44] M. Corvi and W. L. Schaich, Phys. Rev. B **33**, 3688 (1986).
[45] We are using the fact that in the unretarded limit $P_3(z)$ decays to zero if $\omega<\omega_b$ or oscillates if $\omega>\omega_b$ with a length scale much smaller than the optical wavelength, so that the integral $P_3^s=\int P_3(z)dz$ is well defined. This implies that the sum-frequency charge induced at the surface is negligible.
[46] P. Ahlqvist and P. Apell, Phys. Scr. **25**, 587 (1982); C. Schwartz and W. L. Schaich, Phys. Rev. B **26**, 7008 (1982).
[47] N. D. Lang and W. Kohn, Phys. Rev. B **1**, 4555 (1970).
[48] P. J. Feibelman, Prog. Surf. Sci. **12**, 287 (1982); P. J. Feibelman, Phys. Rev. B **40**, 2752 (1989); K.-D. Tsuei, E. W. Plummer, and P. J. Feibelman, Phys. Rev. Lett. **63**, 2256 (1989).
[49] F. Forstmann and R. R. Gerhardts, *Metal Optics Near the Plasma Frequency*, Springer Tracts in Modern Physics Vol. 109 (Springer, Berlin, 1986), Chaps. 2 and 3, and references therein.
[50] A. Liebsch, Phys. Rev. B **36**, 7378 (1987); K. Kempa, A. Liebsch, and W. L. Schaich, *ibid.* **38**, 12 645 (1988).
[51] N. Bloembergen and P. S. Pershan, Phys. Rev. **128**, 606 (1962).